

# HENRY

Hydraulic Engineering Repository

Ein Service der Bundesanstalt für Wasserbau

---

Conference Paper, Published Version

**Rajendra, Kumar; Balaji, Ramakrishnan**

## **Numerical Wave Tank Modeling of Hydrodynamics of Permeable Barriers**

Zur Verfügung gestellt in Kooperation mit/Provided in Cooperation with:  
**Kuratorium für Forschung im Küsteningenieurwesen (KFKI)**

---

Verfügbar unter/Available at: <https://hdl.handle.net/20.500.11970/99437>

Vorgeschlagene Zitierweise/Suggested citation:

Rajendra, Kumar; Balaji, Ramakrishnan (2014): Numerical Wave Tank Modeling of Hydrodynamics of Permeable Barriers. In: Lehfeldt, Rainer; Kopmann, Rebekka (Hg.): ICHE 2014. Proceedings of the 11th International Conference on Hydroscience & Engineering. Karlsruhe: Bundesanstalt für Wasserbau. S. 241-248.

### **Standardnutzungsbedingungen/Terms of Use:**

Die Dokumente in HENRY stehen unter der Creative Commons Lizenz CC BY 4.0, sofern keine abweichenden Nutzungsbedingungen getroffen wurden. Damit ist sowohl die kommerzielle Nutzung als auch das Teilen, die Weiterbearbeitung und Speicherung erlaubt. Das Verwenden und das Bearbeiten stehen unter der Bedingung der Namensnennung. Im Einzelfall kann eine restriktivere Lizenz gelten; dann gelten abweichend von den obigen Nutzungsbedingungen die in der dort genannten Lizenz gewährten Nutzungsrechte.

Documents in HENRY are made available under the Creative Commons License CC BY 4.0, if no other license is applicable. Under CC BY 4.0 commercial use and sharing, remixing, transforming, and building upon the material of the work is permitted. In some cases a different, more restrictive license may apply; if applicable the terms of the restrictive license will be binding.



# Numerical Wave Tank Modeling of Hydrodynamics of Permeable Barriers

K. Rajendra & R. Balaji

*Indian Institute of Technology Bombay, Mumbai, India*

**ABSTRACT:** Breakwaters are structures built to protect the harbour, anchorages or marina basins from the onslaught of ocean waves. In addition, breakwaters enable safe navigation of vessels in and out of a harbour by providing the clam water conditions. Depending on the design requirements, breakwaters can be permeable for better water circulations. In the present study the hydrodynamic performances of single permeable screen are investigated. Experimental and numerical model tests are carried out to estimate the reflection and transmission coefficients of permeable barriers. The details of model, analysis and results are presented in this paper.

*Keywords: Permeable screen, Reflection, Transmission and numerical wave tank*

## 1 INTRODUCTION

In places, where certain degree of transmitted waves is permitted, breakwaters shall be of permeable/porous barriers/screens, which may lead to economical protection from waves in harbors or marinas (Isaacson et al., 1998). It is essential to understand the hydrodynamic characteristics of such permeable screens for efficient design. In general, the wave structure problems are investigated through, analytical, numerical and experimental methods. With increase in the computational infrastructures, numerical models are preferred over experimental model, as they are time consuming and expensive. The analytical methods can be applied to problems with simple mathematical models, geometries and boundaries conditions (Monica et al. 2010). The evolution of Computational Fluid Dynamics (CFD) has opened the window for the development of complex geometry and their dynamic interaction with fluids. The main goal of the present study is to develop a numerical wave tank, using a two dimensional (2D) numerical model based on Volume of Fluid model (VOF) to estimate the hydrodynamic characteristics of permeable barriers. Experimental tests are also carried out to measure the reflection and transmission characteristics of permeable barriers and the same are used to fine tune the numerical wave tank boundary conditions.

## 2 EXPERIMENTAL INVESTIGATIONS

The experimental study is carried out in a 50m long, 0.98m wide and 1m deep physical wave tank facility in the Department of Civil Engineering, Indian Institute of Technology Bombay. One end of the wave tank is installed with a piston-driven wave maker that can generate regular waves of desired periods and heights. A sloping beach is provided at the other end of the wave tank for wave absorption. At the centre of the wave tank, a 5m wide glass wall is fitted to observe the physical phenomenon. Three wave probes are installed on the seaward side of the barrier to measure the composite incident and reflected waves, whereas one wave probe is installed on the leeward side to register the transmitted wave elevations, as shown in Figure 1. The spacing between three wave probes is estimated as per the guidelines of Mansard and Funke (1980). The details of wave train generated inside flume are given in table 1.

Table 1. Details of experimental program.

Water depth ( $d$ , m)	Wave period ( $T$ , sec)	Wave heights ( $H$ , m)
0.5	1.5	0.05, 0.075, 0.1
	1.8	0.05, 0.075, 0.1
	2	0.05, 0.075, 0.1
0.75	1.5	0.05, 0.075, 0.1
	1.8	0.05, 0.075, 0.1
	2	0.05, 0.075, 0.1

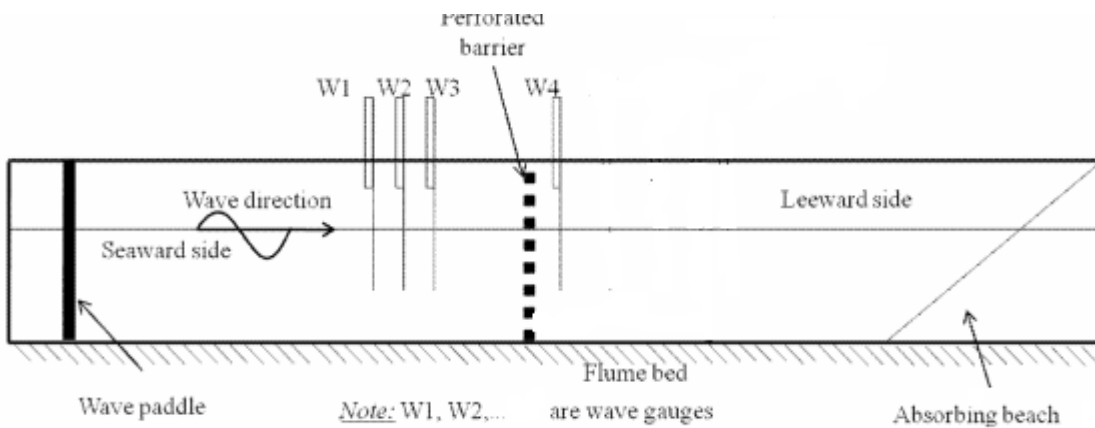


Figure 1. Longitudinal sectional view model setup in wave tank.

### 3 NUMERICAL MODELLING

A numerical wave tank with dimensions similar to the experimental tank is developed, the schematic of which is presented in Figure 2. The perforated barrier model, in terms of boundary conditions, is considered in the middle of the numerical wave tank. A special boundary condition, to represent the piston type wave maker, is used to generate the waves at one end. Similar to physical wave tank, a numerical wave absorber, in terms of slope bed, is adopted at other end of the tank to dissipate the incident wave energy.

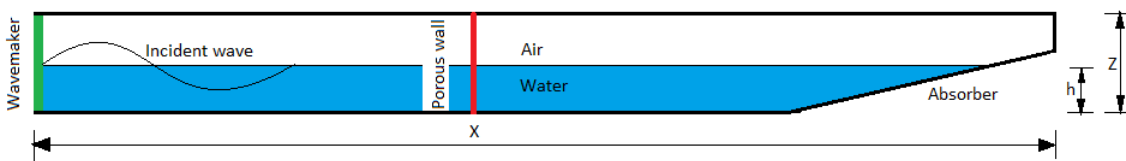


Figure 2. Schematic diagram of numerical wave tank.

The model domain is discretized with quad scheme with map type for rectangular region, and tri with pave for triangular region (slope boundary) as shown in Figure 3. The size of mesh in  $x$  and  $y$  direction is 0.05m respectively, and total number of elements are 19790. With this grid resolution, the total time for CPU processing is 4 hour for wave simulation of 2 minutes.

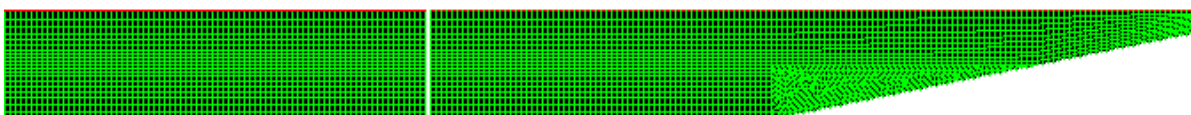


Figure 3. Typical numerical grid for the numerical wave tank.

The two dimensional numerical model, based on Volume of Fluid model (VOF), solves the following continuity and momentum equations.

Momentum equation

$$\frac{\partial u}{\partial t} + u \frac{\partial u}{\partial x} + v \frac{\partial u}{\partial y} = -\frac{\partial P}{\partial x} + \mu \left[ \frac{\partial^2 u}{\partial x^2} + \frac{\partial^2 u}{\partial y^2} \right] \quad (1)$$

$$\frac{\partial v}{\partial t} + u \frac{\partial v}{\partial x} + v \frac{\partial v}{\partial y} = -\frac{\partial P}{\partial y} + \mu \left[ \frac{\partial^2 v}{\partial x^2} + \frac{\partial^2 v}{\partial y^2} \right] \quad (2)$$

Continuity equation

$$\frac{\partial u}{\partial x} + \frac{\partial v}{\partial y} = 0 \quad (3)$$

In which  $P$  = pressure and  $\mu$  = viscosity, and  $u$  and  $v$  are velocities in two coordinate systems  $x$  and  $y$  respectively.

The numerical wave tank is imposed with four different surrounding boundary conditions, as described in Figure 2. The inlet left boundary is controlled by the wave maker motion, the displacement of which is given by;

$$\frac{H_0}{2e} = \frac{4 \sinh^2 kd}{2kd + \sinh 2kd} \quad (4)$$

Where;  $H_0$ =Wave height,  $e$ =Amplitude of wave maker displacement,  $d$ =Water depth and  $k$ =Wave number.

The bed of the numerical wave tank is imposed with wall boundary condition, in which the normal gradient of potential function should vanish, as;

$$\frac{\partial \phi}{\partial n} = 0 \quad (5)$$

The thin porous medium has a finite thickness over which the pressure change is defined using viscous loss and inertial losses (Ansys 2009). The porous boundary condition for the case of simple homogeneous porous media is given as;

$$\Delta P = -\left( \frac{\mu}{\alpha} \mathfrak{G}_i + C \frac{1}{2} \rho |v| v_i \right) \Delta m \quad (6)$$

Where,  $\Delta P$  = Pressure difference,  $\Delta m$  = thickness of medium,  $\alpha$  = Permeability,  $C$ = Inertial Resistance factor,  $\mu$  = Laminar fluid flow,  $v$  = Velocity normal to the face.

The wave characteristics inside the numerical wave tank are controlled by the maker boundary conditions and the reflected and transmitted waves off permeable boundary are controlled by the inertial resistance coefficient. The boundary condition is summarized in table 2 along with other parameters setting applied in numerical model.

Table 2. Assignment of boundary conditions and parameters setting

Region	Boundary Conditions
Top Boundary	Pressure outlet
Bottom Boundary	Wall
Left Boundary	Moving wall
Right Boundary	Wave absorber (Slope 1:5)
Solver	Segregated
Multiphase	VOF
Pressure	Presto
Momentum	First order upwind
Volume Fraction	First order upwind
Scheme	Non-iterative time advancing
Discretization scheme	First-order upwind
Mesh deformation scheme	Dynamic mesh
Precision	Double

#### 4 RESULTS AND DISCUSSION

To start with, monochromatic regular waves are generated in the numerical wave tank, without considering the permeable barrier, a snap shot of which is shown in Figure 4. Further, typical wave elevations, extracted along various locations along the tank, as shown in Figure 5, also demonstrated that the numerically simulated waves do not decay, in the present study. The wave elevations, extracted at a particular section of the numerical wave tank is then compared with that of linear wave theory, as typically shown in Figure 6, and found to be in agreement.

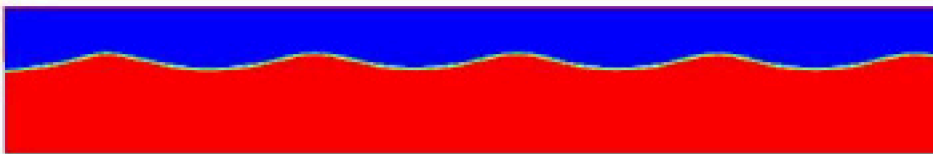


Figure 4. Typical generation of waves in the numerical wave tank ( $H=0.05\text{m}$ ,  $T=2\text{s}$ ).

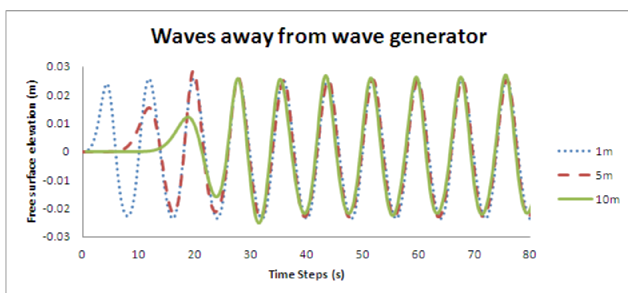


Figure 5. Wave elevations at various locations along the length of numerical wave tank ( $X=1$ ,  $X=5$  and  $X=10\text{m}$  from wave maker,  $H=0.05\text{m}$ ,  $T=2\text{s}$ ).

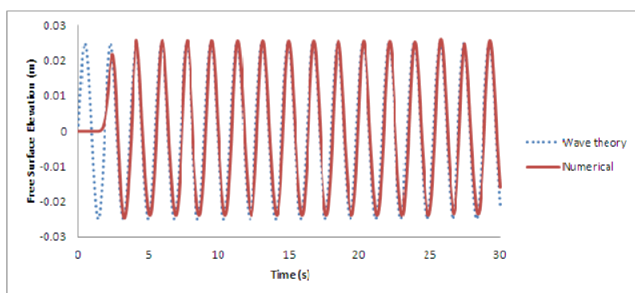


Figure 6. Typical comparison of wave elevations ( $H=0.05\text{m}$ ,  $T=1.8\text{s}$ ).

Further, the permeable boundary condition is then introduced in the numerical model and the wave elevations are extracted at locations similar to experimental program. Four different porosities (5%, 10%, 15%

and 20%) of the permeable screens are considered for the present study in a constant water depth,  $d$  of 0.5m. The inertial resistance coefficient is adjusted in the permeable boundary condition, so as to match with the experimentally measured wave elevations.

The wave elevations estimated from the numerical wave tank is compared with that of obtained from experiments, as typically shown for  $d=0.5\text{m}$ ,  $P=20\%$  and  $H/L=0.0265$  in Figure 7, clearly demonstrates the agreement. The typical wave elevations shown in that figure are extracted on the seaward and leeward side of the permeable barrier. It is clear from the figure that the numerical model capable of estimating the reflected and transmitted wave elevations.

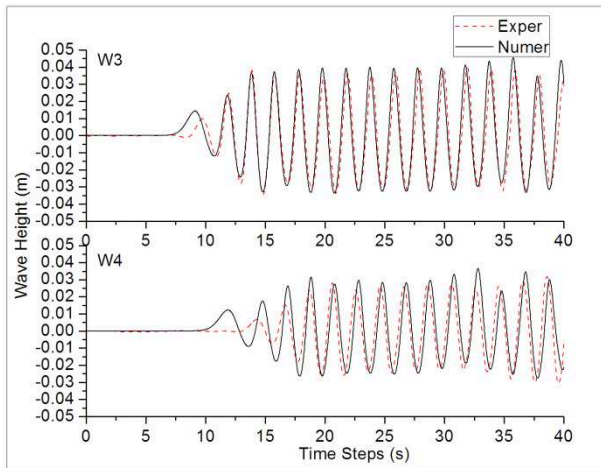


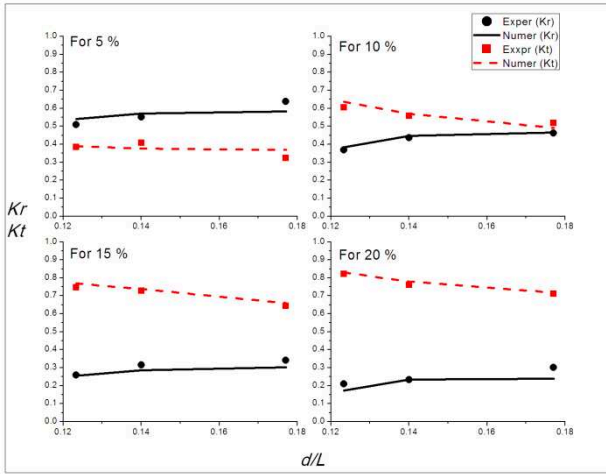
Figure 7. Time series comparison with experimental studies for  $H/L=0.0265$  and  $P=20\%$ .

#### *Reflection and Transmission characteristics*

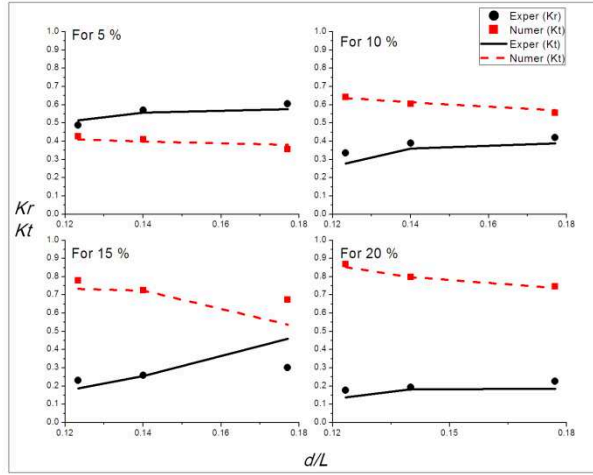
Both experimental and numerical wave elevations obtained from the three seaward probes were subjected to analysis to get the average reflection coefficient,  $Kr$ . The wave elevations measured on the leeward side of the barrier are subjected to statistical analysis to the transmitted wave height, which is then normalised with incident wave height to get the transmission coefficient,  $Kt$ . The variation of  $Kr$  and  $Kt$  with relative water depth,  $d/L$  for different porosities are shown in Figure 8. It observed from the figures that  $Kr$  increases with increase in  $d/L$  for all three wave heights, due to the fact that the shorter waves are reflected back without getting attenuated. Higher reflections of waves are observed for lesser barrier porosity, as they offer more resistance to the flow of waves through it. The  $Kt$  is observed to be decreasing with increase in  $d/L$ , due to the fact that the longer waves are past the barrier without significantly reflected from the barrier.

The variation of  $Kr$  and  $Kt$  with porosity for a particular wave period,  $T=1.5\text{s}$ , shown in Figure 9, demonstrates the effect of porosity on the reflection and transmission wave characteristics. It is observed from the figures that the numerical model capable of predicting the hydrodynamics of permeable barriers.

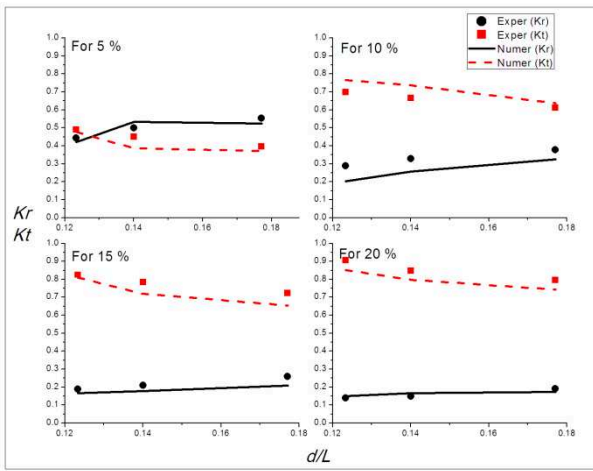
As mentioned earlier, the inertial resistance coefficients on the permeable boundary conditions, eqn. (6) are adjusted by trial and error method, for each of the barrier porosity to obtain wave elevations close to that of experimentally measure elevations. An attempt is made in the present study, to explore the relation between the resistance coefficient and the barrier porosity. The final inertial resistance coefficients obtained for all the tested barrier porosities are shown in Figure 10. It is observed from the figure that the resistance coefficient decreases with increase in barrier porosity, as observed in the experiments. It is also observed that the resistance to the waves through the permeable barriers increases with increase in wave steepness, as seen in Figure 10b.



(a)  $H=0.1m$



(b)  $H=0.075$



(c)  $H=0.05m$

Figure 8. Variation of  $K_r$  and  $K_t$  with  $d/L$ .

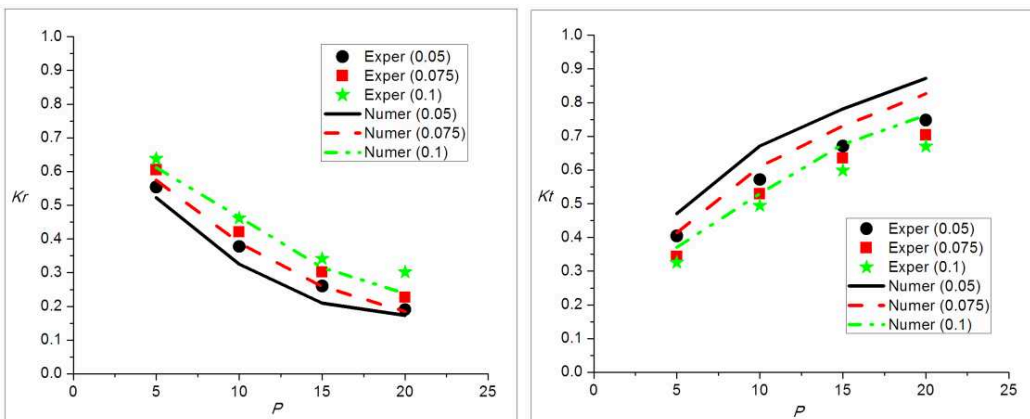
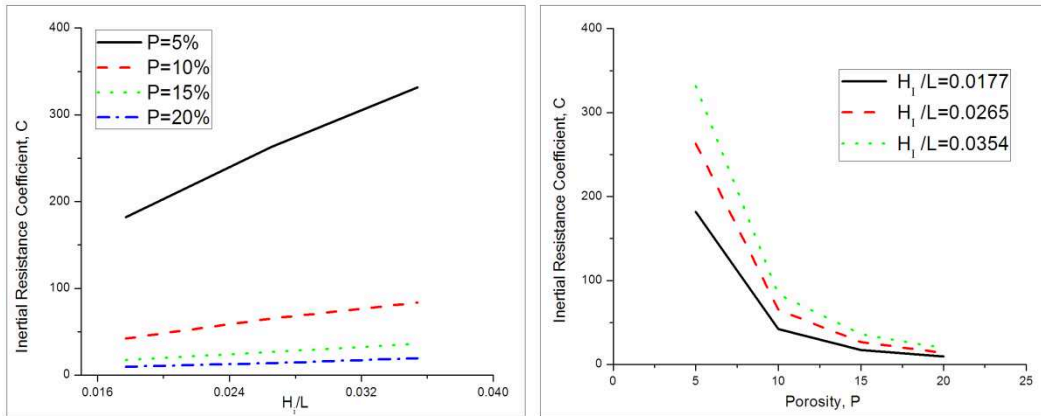


Figure 9. Variation of reflection and transmission with porosity of the barrier.



(a) effect of porosity (b) effect of wave steepness

Figure 10. Variation of inertial resistance coefficient.

## 5 CONCLUSION

A numerical wave tank is developed to estimate the hydrodynamics of permeable barriers. The reflection and transmitted wave elevations obtained from the numerical wave tank are compared with that obtained from an experimental investigation and found to be in agreement. The inertial resistance coefficients, representing the permeable boundary conditions in the numerical wave tank, are obtained by comparing the wave elevations of experimental program. A relationship between the barrier porosity and the inertial resistance coefficients is also established through the present study.

## REFERENCES

- ANSYS-Inc., 2009. ANSYS CFX, Release 12.1. 2009.
- Isaacson, M., Premasiri, S., Yang, G., (1998). Wave interactions with vertical slotted barrier. *Journal of Waterway, Port, Coastal, and Ocean Engineering* 124 (3), 118–126.
- Mansard, E. P. D. & Funke, E. R., 1980. “The measurement of incident and reflected spectra using a least squares method.” In *Proc. 17th Coastal Eng. Conf., Sydney, Australia*, pp. 159-174.